GEOPHYSICS, VOL. 62, NO. 3 (MAY-JUNE 1997); P. 842–852, 10 FIGS.

Hydrophone VSP imaging at a shallow site

Paul A. Milligan*, James W. Rector III‡, and Robert W. Bainer**

ABSTRACT

We evaluated the capabilities of vertical seismic profiling (VSP) for imaging the complex heterogeneous unconsolidated sedimentary structures at a shallow site. We deployed a 24-level hydrophone array with 0.5-m level spacing down a preexisting poly vinyl chloride (PVC) cased well. Data acquisition time was quick. Only 15 multioffset shot points using a hammer-on-plate source were needed to acquire reflection data between the water table at 3 m and the bedrock at 35 m to produce a depth section image. This image extended 9 m from the receiver well, yielding resolutions between fresh-water–bearing sands and impermeable muds and clays of better than 1 m. Depth accuracy of the image was confirmed by good correlation with cone penetrometer logs. We used conventional wavefield separation and VSP-CDP mapping techniques to image the data.

Tube waves, created by seismic arrivals at cross-sectional area changes in the borehole fluid column, were the primary source of coherent noise in the data. The tube-wave arrival structure was complicated by the hydrophone array, which generated and scattered tube waves at each hydrophone pod. To combat the tube wave interference, we inserted closed-cell-foam baffles between elements. The baffles attenuated and slowed the tube waves, and reduced generation and scattering. A comparison between unbaffled and baffled VSP data showed that baffling increased the maximum useful frequency from 300 Hz to over 900 Hz. By contrast, surface shot data recorded at the same site, using buried 40-Hz vertical geophones, exhibited useful frequencies of less than 250 Hz. In addition, coherent noise in surface shot records caused by air waves and first arrivals made it very difficult to identify shallow reflections above 25 m. Reflections from depths as shallow as 10 m were easy to identify in the baffled VSP data.

INTRODUCTION

Surface reflection techniques have been used to image the geologic structure of the first 20–50 m of the subsurface (Hunter et al., 1984; Steeples et al., 1988; Matsubara et al., 1994). However, surface reflection techniques have limitations when attempting to image small-scale structures at very shallow depths. One impediment to using surface seismic for near-surface reflection imaging is the masking of reflection events by strong coherent noise, such as air waves, ground roll, shallow refractions, and guided waves, traveling very near the surface (Hunter et al., 1984; Steeples et al., 1988). Consequently, muting above 20 ms to exclude first break refraction arrivals is common (e.g., Doll et al., 1994; Matsubara et al., 1994), and airwave plus ground-roll contamination of the near offset traces often makes precritical incidence-angle reflection events at shallow depths unobtainable.

In addition, geophones planted at the surface typically exhibit a frequency response that severely attenuates signals above 200–300 Hz (Krohn, 1984). Krohn et al. (1991) showed that burial of geophones 1 m below the surface could increase useful frequency response by up to 40 Hz, and Herridge (Herridge, B. J., 1994, personal communication) collected data with a maximum frequency of over 300 Hz using geophones that were rigidly coupled (without spikes) to asphalt in a bay-fill environment. However, both burial or fixing of geophones to a hard surface requires more acquisition time and increased costs.

Vertical seismic profiling (VSP) is a viable alternative to using surface techniques for imaging subsurface structures. In this study, we evaluate VSP reflection imaging using a multilevel hydrophone array at a bay margin site with shallow boreholes [total depth (TD) less than 70 m]. VSP has been used for many years as a calibration tool for surface seismic data (Hardage, 1983). However, it is seldom used as a stand-alone imaging tool in deep wells because the combined cost of rig time, hole risk, and the multiple source offsets required for imaging can be quite high. However, *near-surface* structure imaging appears to be well-suited to the VSP method, especially when using

Manuscript received by the Editor July 13, 1995; revised manuscript received August 5, 1996.
*Engineering Geoscience, Building 90, Room 2002, Lawrence Berkeley National Laboratory, University of California, Berkeley, California 94270.
‡Department of Materials, Science & Mineral Engineering, University of California at Berkeley, 577 Evans Hall, Berkeley, California 94270.
**Environmental Restoration Division, MS L619, 7000 East Avenue, Lawrence Livermore National Laboratory, Livermore, California 94551.
© 1997 Society of Exploration Geophysicists. All rights reserved.

a multilevel hydrophone array as the imaging tool. Borehole clamping geophone tools are often expensive and difficult to use, usually with fewer than six receiver levels, requiring repositioning of the tool many times while repeating the same shotpoints. By using a simple weight-drop source and a multilevel hydrophone array, multioffset VSP data can be collected quickly and efficiently. At many environmental clean-up sites, shallow boreholes are often available, and, if not, can be easily drilled in largely unconsolidated sediment.

Like other investigators (Marzetta and Schoenbeig, 1985; Marzetta et al., 1988; Krohn and Chen, 1992), we found that tube waves were the principal noise components in the hydrophone VSP data. The tube wavefield was complicated by generation and scattering off the hydrophones. With the use of interhydrophone closed-cell foam baffles, we were able to substantially attenuate and slow the tube waves, which resulted in a significant increase in the bandwidth of wanted signals (i.e., direct and reflected *P*-wave arrivals). Reflection images produced from the baffled data exhibited high resolution (better than 1 m) and correlated well with cone penetrometer logs. By contrast, surface shot records (at the same site) were contaminated by coherent noise in the form of air wave, ground roll, and first-arrival refraction interference, and exhibited frequency content that was substantially lower than the VSP data.

SITE DESCRIPTION AND DATA ACQUISITION

We collected multioffset hydrophone VSP data, and surface seismic data at the Richmond Field Station, located about 300 m from San Francisco Bay near Richmond, California. This site consists of unconsolidated quaternary clastics, extending from the surface down to the Franciscan basement at a depth between 30 and 40 m (Pouch, 1987). The recent depositional environment is fresh deltaic, with bay muds interleaved with thin sand and gravel layers and lenses. The mean water table depth was about 3 m.

The experiment site contained nine boreholes that were available for the VSP study, over about a 50-m square area. We chose a borehole with a TD of 70 m, and cased with 6-inch (152-mm) PVC pipe that was not cemented. Figure 1 shows a north-south stratigraphic cross-section that was produced from drilling logs and pump tests at this site (Pouch, 1987). The borehole we used for the VSP survey is located near the center of the cross-section. Pump tests indicated no common aquifer connection between most wells at this site. Note the lack of continuous units below 12 m, indicating the lateral heterogeneity of the site.

For the VSP survey, we used a 24-level, 0.5-m spaced hydrophone array with built-in preamplifiers that was specifically designed for shallow boreholes. We initially tested both

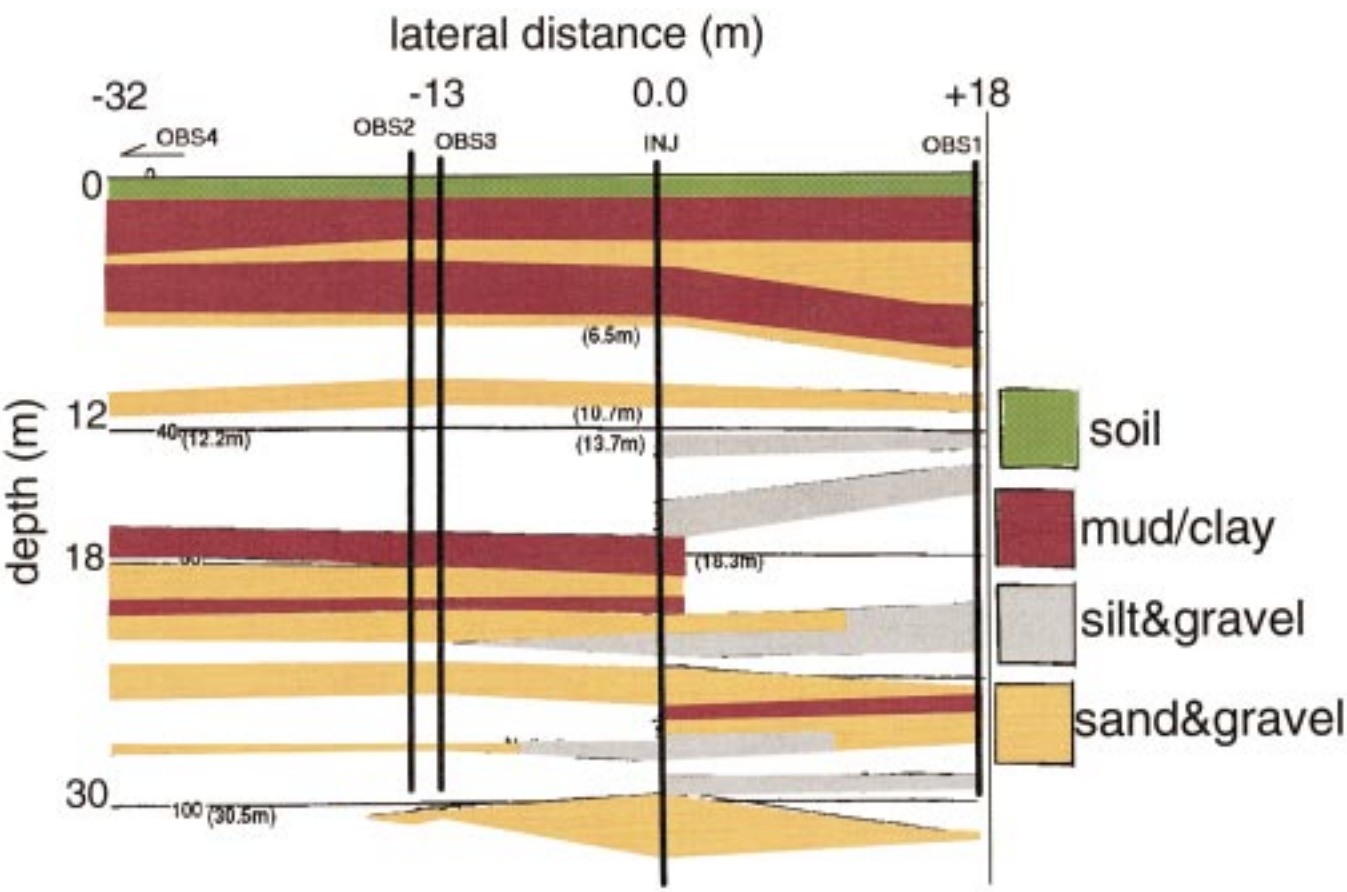

FIG. 1. North-south lithologic cross-section at the Richmond Field Station based on well logs and pumping tests (Pouch, 1987). The VSP well was 2 m southwest of well INJ.

a hammer-on-plate source and a Betsy Gun source that fired 12-gauge blanks down a 1-m auger-drilled and water-filled hole. We found little difference in frequency content and signal-to-noise ratio (S/N) between the Betsy Gun data and the hammer-on-plate data. Typically, we found that 5–6 hammer blows were comparable to the S/N of a single Betsy Gun shot.

We used the hammer-on-plate source to collect multioffset VSP data. Shotpoints were located at 1.2-m intervals along a radial line from the wellhead to a maximum offset of 18 m. For each shotpoint, we recorded 48 receiver levels between 5.0 and 28.5 m, which required one, 12-m move of the hydrophone array and repetition of all 15 shotpoints. The hammer-on-plate source shortened data acquisition time considerably compared to the Betsy Gun, which would have required augering of two shot holes for each shotpoint. The total acquisition time to deploy the array and record 30 VSP shot records (720 traces) was less than 4 hours.

From the initial analysis of VSP records, we determined that tube waves were the major coherent noise source, leading to difficulty in separation of reflection wavefields. To attenuate the tube waves, we added closed-cell foam baffles (Pham et al., 1993) to fill the gaps between each hydrophone level. We also extended the foam about 1.5 m above the first level and between the last level and the tail-end weight. The closed-cell foam was in the form of 0.5-inch (12.5-mm) pipe insulation sections that were cut to size and taped onto the cable between the hydrophones. The baffles had an outside diameter (44 mm) similar to that of the hydrophones and the tail-end weight, which helped to reduced tube wave generation and scattering from cross-sectional area changes in the borehole fluid column (Hardage, 1981, 1983).

We collected surface shot records from a surface geophone array to compare with the VSP data. Common shotpoint gathers were collected in a walkaway noise geometry, using offsets between 3 and 63 m, and a 0.5-m geophone spacing. To reduce wind noise and improve coupling, we buried each geophone about 10 cm. We tested both sources, and found that a single Betsy Gun shot produced higher S/N than a stack of ten hammer blows, yielding broader bandwidth and significantly lower levels of air wave and ground roll interference. We used the Betsy Gun data in subsequent comparisons with hammer-on-plate VSP data. With the 24-channel recording equipment available, it took us two days to acquire six 120-trace common shotpoint gathers (20 Betsy shots, 10 hammer positions; 720 total traces).

COMPARISON BETWEEN SURFACE GEOPHONE DATA AND HYDROPHONE VSP DATA

Figure 2 shows a surface common shotpoint gather (CSG) using the Betsy Gun both before (Figure 2a) and after (Figure 2b) 80 to 600 Hz bandpass filtering and deconvolution. Filtering attenuated the low-frequency ground roll modes dominating the raw records. The principal arrivals in Figure 2b are the first breaks and the shot-generated air wave. Hyperbolic reflection

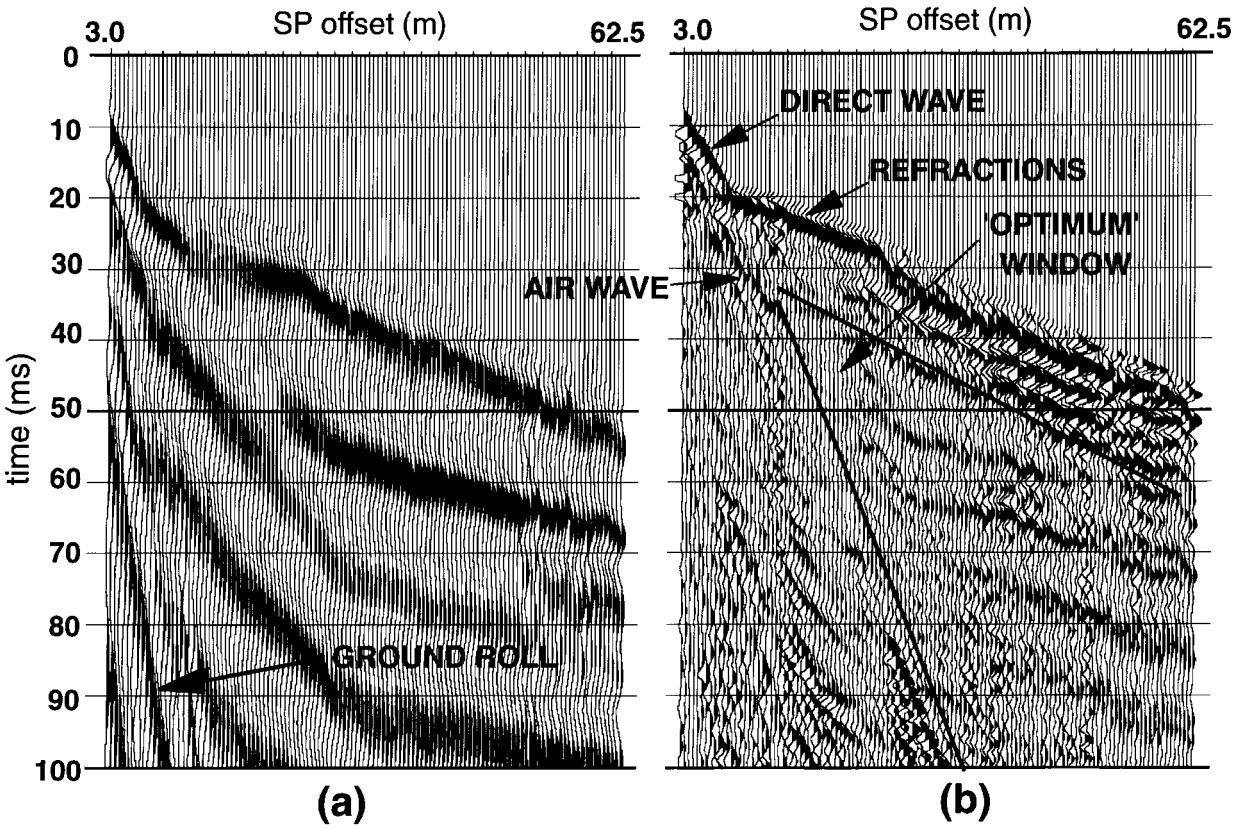

FIG. 2. Surface CSG (120 trace) using Betsy Gun source and 40-Hz vertical geophones buried 10 cm: (a) raw data with automatic gain control (AGC), (b) after bandpass filtering (80 to 600 Hz) , AGC, and deconvolution. Geophone spacing is 0.5 m. The "optimum" window in which to look for reflection events, uncontaminated by airwaves and refractions, is shown.

arrivals can only be reliably detected within an "optimum" time/offset window between the air waves and the first breaks (Hunter et al., 1984). The optimum window in Figure 2b limits its useful reflection times to those greater than 35 ms (roughly 25 m). At traveltimes less than 35 ms, reflection arrivals are obscured by air waves (at the near offsets) and first break energy (at the longer offsets). Even with CMP stacking improvement, reflection events from traveltimes less than 35 ms may be obscured by shot-generated noise.

Large static shifts in the first break time are apparent in Figure 2, particularly at the longer offsets. Note the short (12–25 m offset) subset of first breaks that do not appear to have much significant time jitter; these offsets correspond to a well-packed gravel road. We believe that the statics are caused by lateral velocity variations in the first meter of unsaturated soil, where the P-wave velocity may drop below 330 m/s (Krohn et al., 1991; Steeples et al., 1988). CMP processing of this data would require accurate static corrections to ensure adequate stack performance at higher frequencies. In VSP, shotpoint static corrections can be accurately estimated from the direct-wave first-break picks.

Figure 3a is an unprocessed VSP CSG, collected using the interlevel foam baffles from an offset of 7.2 m. The principal arrivals in Figure 3a are direct waves and tube waves. The two strong upgoing tube wave arrivals coincide with the direct arrival near the deepest hydrophone element in each 24-level gather, confirming that body waves convert to tube waves at cross-sectional area changes in the fluid column. Figure 3b shows the data in Figure 3a after a 140 to 1200 Hz band-pass filter, AGC, and deconvolution. The filtering has attenuated the tube waves and has revealed substantial bandwidth in the other arrivals. Unlike the surface shot records, where shallow reflections were obscured by coherent interference, upgoing reflection arrivals from depths between 10 and 30 m can be clearly seen in the VSP data, with a dominant period of about 1.6 ms.

The f-k spectra of the surface CSG and the VSP CSG (Figures 4a and 4b, respectively) show that the maximum frequency in the VSP data (over 900 Hz) is about four times the maximum useful frequency in the surface data. In the surface f-k spectrum (Figure 4a), there are high-amplitude zones corresponding to the first breaks (and, possibly, weaker reflections) and the air wave. The apparent velocity of the first breaks is between 1600 and 3000 m/s, whereas the apparent velocity of the airwave is 330 m/s. The maximum usable frequency for the high-velocity arrivals of interest is less than 250 Hz, whereas the undesired airwave arrival has a maximum frequency of more than 400 Hz and exhibits spatial aliasing at the higher frequencies. By contrast, in the VSP f-k spectrum (Figure 4b), we see both direct (positive wavenumbers) and reflected (negative wavenumbers) arrivals with a maximum frequency over 900 Hz.

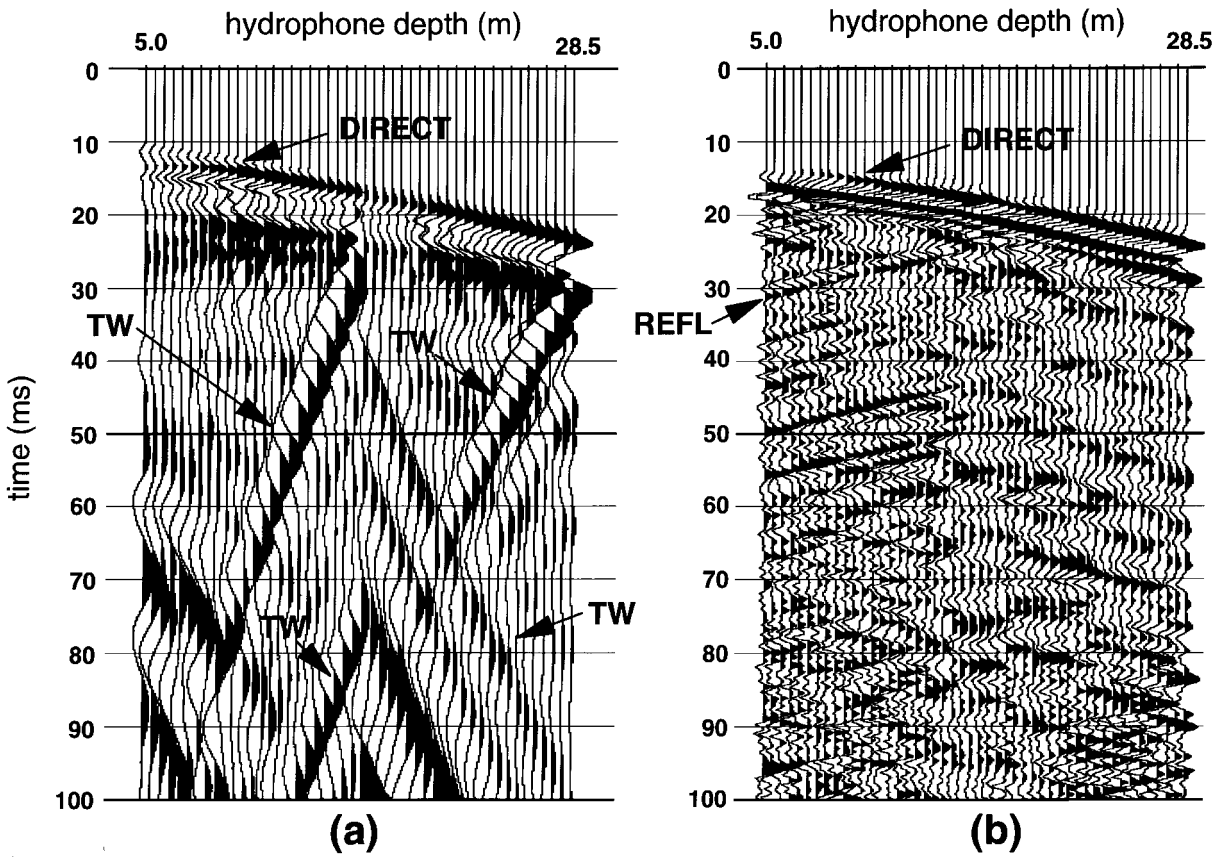

FIG. 3. Baffled hydrophone VSP CSG (48 trace) from hammer-on-plate source at offset 7.2 m: (a) raw data with AGC, (b) after bandpass filtering (140–1200 Hz), AGC, and deconvolution. Hydrophone spacing is 0.5 m. Reflection events are labeled REFL, tube wave events are labeled TW, direct wave is labeled DIRECT.

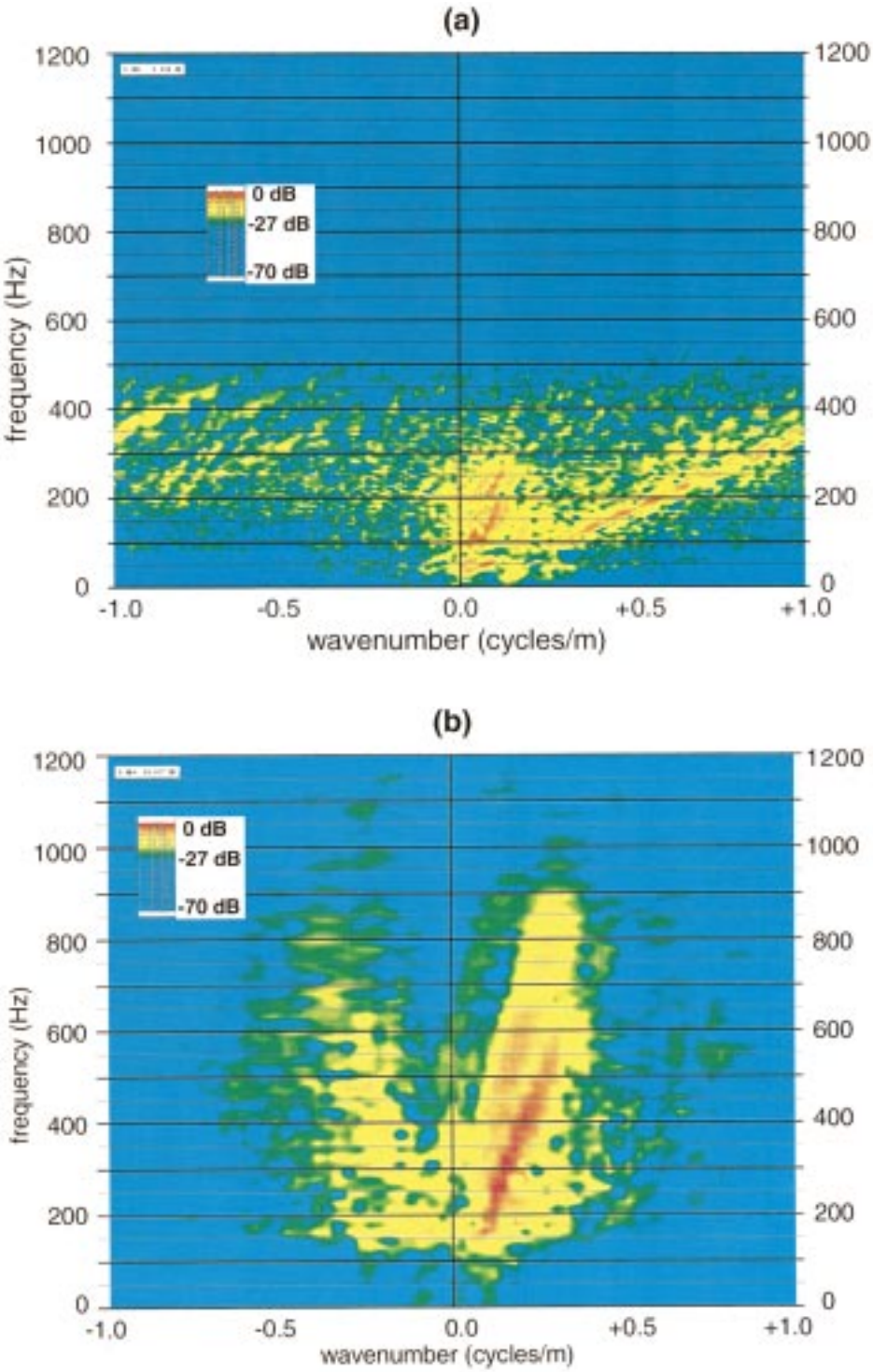

FIG. 4. The f-k spectra of: (a) surface shot gather, 120 trace, (b) VSP shot gather, 48 trace. Note that the bandwidth of the baffled hydrophone VSP data is over four times that of the surface geophone data.

As a result of these comparisons, we determined that the hydrophone VSP data using interlevel foam baffles were superior to the surface geophone data in terms of S/N and bandwidth. The VSP data exhibited reflections from depths shallower than 25 m, whereas in the surface CSG data, these shallow depths were obscured by shot-generated noise.

TUBE-WAVE SUPPRESSION USING INTERHYDROPHONE BAFFLES

Figure 5a is a raw VSP shot record without any closed-cell foam baffles. Very strong tube waves are present (velocity 630 m/s) which dominate all other arrivals, including the direct wave. The strongest tube wave is generated by the *P*-wave direct arrival when it hits the top of the fluid column (at 3 m). We can also see a reflection of this primary tube wave off the tail end of the hydrophone array and off the bottom of the borehole.

Figures 5b and 5c show a shot record with the same geometry as Figure 5a, but with foam baffles added between each hydrophone down to hydrophone 17 (the cables between hydrophones 17 to 24 were left bare). True relative amplitude has been maintained between Figures 5a and 5b, whereas Figure 5c has had its traces individually scaled for clarity. In Figure 5b, note the substantial decrease in both tube wave and direct-arrival amplitude where baffles have been inserted. The tube waves have been attenuated by nearly 20 dB, while the direct arrival has been attenuated by about 10 dB. We believe that the tube wave attenuation is caused by absorption inside the air-cell matrix of the baffles.

In Figure 5c, we can see how the baffles affected the bandwidth and velocity of the tube waves. Note that the downgoing tube wave from the top of the fluid column has been slowed to a velocity of about 130 m/s, roughly one-fifth of the unbaffled tube-wave velocity. The downgoing tube wave also has a period that is 1.5–2 times larger than the unbaffled tube-wave period, indicating a decrease in frequency bandwidth. Where the baffles stop at hydrophone 17 (13 m depth in Figure 5c), both upgoing and downgoing tube waves have been generated; the downgoing tube wave travels past the unbaffled hydrophones at full velocity (630 m/s), while the upgoing tube-wave velocity has been reduced to 130 m/s.

The conversion of direct *P*-waves to tube waves at the top and bottom of the fluid column, at the bottom of the hydrophone array, and at the end of the baffled section are in agreement with Hardage (1981, 1983). Hardage showed that changes in the cross-sectional area of the fluid column act as efficient coupling points between body waves in the formation and tube waves in the borehole. Kurkjian (1986) showed that the coupling coefficient was proportional to the cross-sectional area change of the fluid column and that, in general, coupling coefficients due to cross-sectional area changes were much larger than coupling coefficients due to lithology changes adjacent to the borehole. By inference, the top and bottom edges

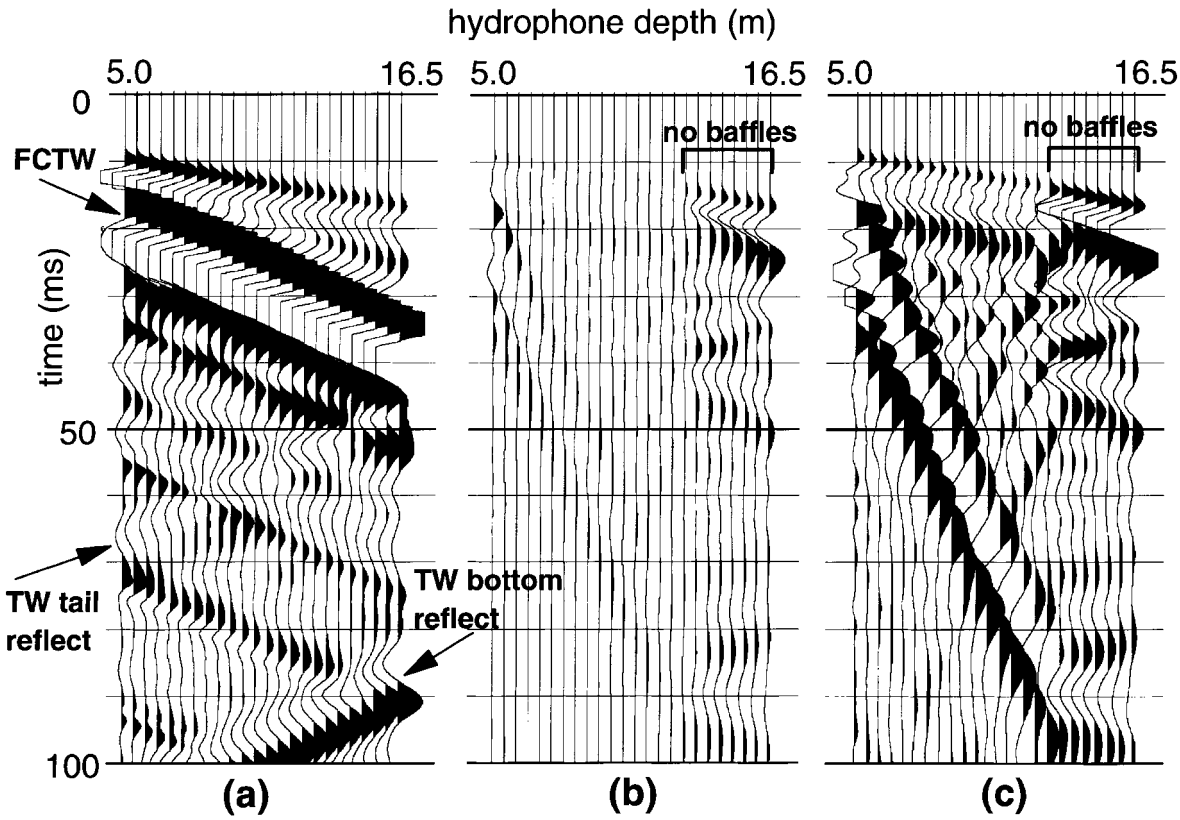

FIG. 5. Raw VSP shot record, 24 trace: (a) without baffles, (b) with interhydrophone baffles, (c) baffled, but with individual trace normalization. Note that hydrophones below No. 17 were left unbaffled. "FCTW" indicates the tube wave generated at the top of the fluid column, "TW tail reflect" indicates the tube wave reflected from the tail of the hydrophone array, and "TW bottom reflect" indicates the tube wave reflected from the borehole bottom.

of each hydrophone element, which have roughly a 3-cm diameter contrast with the hydrophone cable, are also coupling points. The interhydrophone baffles were selected to have a diameter nearly equivalent to the hydrophone element, thus reducing the coupling coefficient.

One of the most useful by-products of using baffles is a dramatic increase in the bandwidth of the direct P-wave arrival. This is illustrated in Figure 6, which compares the f-k spectra of the unbaffled hydrophone array (Figure 6a) and the baffled array (Figure 6b). There has been a 500-Hz increase in bandwidth of the direct wave arrivals in the positive wavenumber quadrant for the baffled array, and some reflection energy with a similar bandwidth can be seen in the negative quadrant. Without baffles, the useful frequency content of the VSP data is comparable to that of the surface geophone data.

We believe that the loss of P-wave high frequencies in the unbaffled data is primarily due to interference from tube-wave arrivals. A diagram of the hypothesized tube-wave interference is shown in Figure 7. At time t_0, the incident wavefront intersects the receiver level of interest and creates a "primary" arrival. Tube waves, generated at the edges of nearby hydrophone elements, arrive at this receiver delayed in time $(t_0 + \Delta t_i)$ when the apparent velocity of the incoming body wave exceeds the tube-wave velocity. The first four tube-wave arrivals are labeled in chronological order (Δt_1 to Δt_4) in Figure 7. The summation of the primary arrival with the delayed tube-wave arrivals low-pass filters the primary waveform, provided the time delays are comparable to the dominant half-period of the primary. The filter characteristics will change as a function of the Δt_i values, which are dependent on incidence angle, tube wave velocity, and hydrophone element spacing.

Figure 8 illustrates the effect of depth on the performance of the foam baffles. At deeper borehole levels, the baffling was less effective at slowing and attenuating the tube waves. Increasing hydrostatic head pressure collapsed the baffle's air cells, reducing their ability to absorb and dissipate the tube waves as effectively. The baffled tube-wave velocity starts at 106 m/s for the shallowest level (3 m) and increases to 620 m/s for the deepest level (85 m). A foam material with a stiffer bulk modulus and/or higher air-cell pressure would be needed at deeper levels.

REFLECTION IMAGING OF THE BAFFLED MULTIOFFSET VSP DATA

To evaluate the reflection imaging capability of the baffled, multioffset hydrophone VSP data, we used conventional VSP processing, consisting of wavefield separation (e.g., Glangeaud and Mari, 1994) and reflection mapping using the VSP-CDP transform (e.g., Wyatt and Wyatt, 1981; Cassell et al., 1984). Wavefield separation was employed to attenuate upgoing and downgoing tube waves and downgoing direct waves. A combination of low-cut filtering (140 Hz cutoff frequency) and f-k fan filtering was used to attenuate the low-frequency, low-velocity tube waves. To remove the downgoing arrivals, we compared different multichannel filters (median, f-k, τ-p, and eigenvector) applied after direct arrival alignment and equalization. The eigenvector filter (Glangeaud and Mari, 1994) yielded results with the smallest edge effects. The common receiver domain was also used in the wavefield separation processing because of the 1.2-m shotpoint spacing. After wavefield separation, we deconvolved the source signature, which widened the frequency spectrum of the reflected arrivals.

We used VSP-CDP mapping applied to each CSG to image the wavefield-separated reflections. The nearest shotpoint offset (1.2 m) was too close to the well for adequate reflection signal strength, so we only stacked offsets between 2.4 and 18 m. The VSP-CDP transform algorithm assumed a 1-D layered earth model and incorporated ray bending at interfaces (Lazaratos, 1993). A 2-D structure can be handled with more advanced VSP-CDP algorithms or with VSP migration (Cassell et al., 1984; Payne et al., 1994). However, at this site, there was no dominant dip trend, and the heterogeneities were expected to be fully 3-D in nature. Imaging of 3-D structure would require multiazimuth shotpoints and 3-D migration.

For each shotpoint, the VSP-CDP mapping velocity field was estimated from the first breaks. The only significant shotpoint-to-shotpoint velocity variations that we found were in the very near surface (0–5 m) or at very wide angles (i.e., large shotpoint offsets and very shallow receiver depths). Consequently, to obtain a mapping velocity function for each shotpoint, the velocities obtained from the nearest three offsets were averaged to obtain a shotpoint-*independent* velocity field for depths below 5 m, then a shotpoint-*dependent* velocity was estimated between 0 and 5 m based on the first break statics. After VSP-CDP mapping the individual CSGs, the resulting depth sections were stacked after amplitude balancing and minor vertical alignment (less than 0.2 m).

Figure 9 shows the interval velocity versus depth function for the three nearest offsets, along with an induction log from the VSP well and a driller's log from a nearby (2-m offset) well. Figure 10 is the stacked reflection image. There is a correlation between P-wave velocity peaks and induction log peaks (high resistivity), which correlate with gravel/sand units in the driller's log. These units are interpreted to be fresh water aquifers.

Logs from two cone penetrometer tests (Robertson and Campanella, 1983) (CPT1 and CPT4) have been spliced into the reflection image of Figure 10. The logs consisted of bearing load, sleeve friction, and DC resistivity. Increasing darkness in the CPT log traces means higher bearing load, higher sleeve friction, and higher resistivity. A zone of fresh-water–saturated sand or gravel is indicated when all three of these parameters are high (dark). The CPT1 hole stopped at 21 m while trying to penetrate a gravel/sand layer. The 21-m depth corresponds with a major reflection horizon in the stacked section, a high-velocity zone in Figure 9, a dark interval in both CPT logs, and a gravel/sand layer interpreted from the driller's log. There is also good correlation between the stacked section and CPT1 at other depths, with interpreted aquifers at 11.0 and 12.5 m. The 11-m reflection horizon correlates well with CPT1, but as wellhead offset increases, we see a slight dip (about 6°) on the horizon and a mistie of about 0.5 m with CPT4. The mistie could be due to minor elevation variations between the wellhead and the top of the CPT4 hole. Neither CPT log was surveyed to a common elevation datum. There is a steep down-dipping (about 30°) event at 16 m that is quite strong at zero offset but fades out after 5 m. This event does not seem to correlate with any significant deflections in the CPT1 logs. This event could be a diffraction, a converted arrival, or an out-of-plane arrival. Of particular interest in the reflection image is the apparent pinch-out of a reflector at 28 m, less than 1 m away from the well.

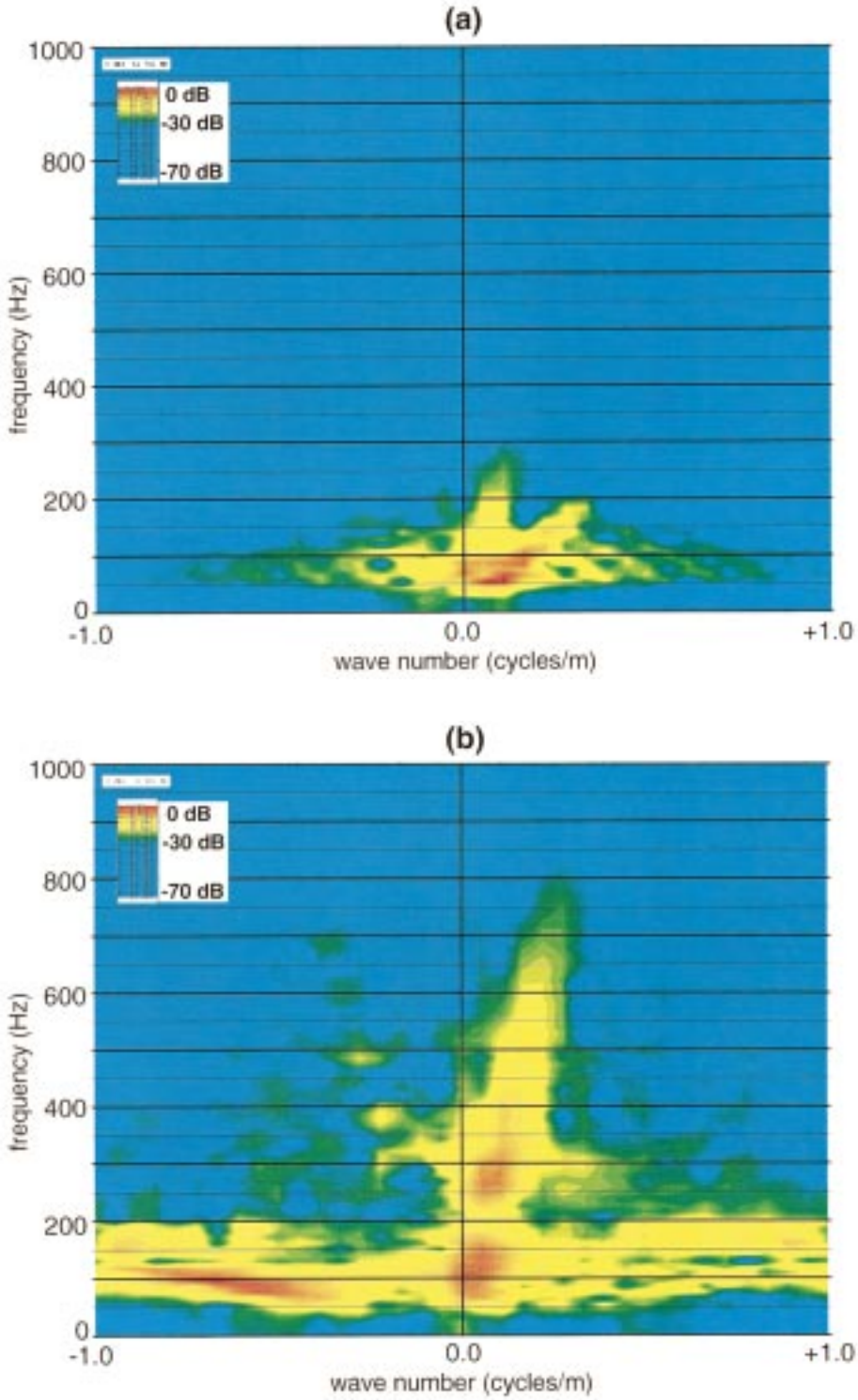

FIG. 6. The *f-k* spectra of raw, 24-trace VSP shot records (a) without baffles, (b) with interhydrophone baffles. Note the 500-Hz increase in bandwidth of the direct arrivals in the baffled data set, together with a reduction in tube wave velocity from about 600 to 130 m/s.

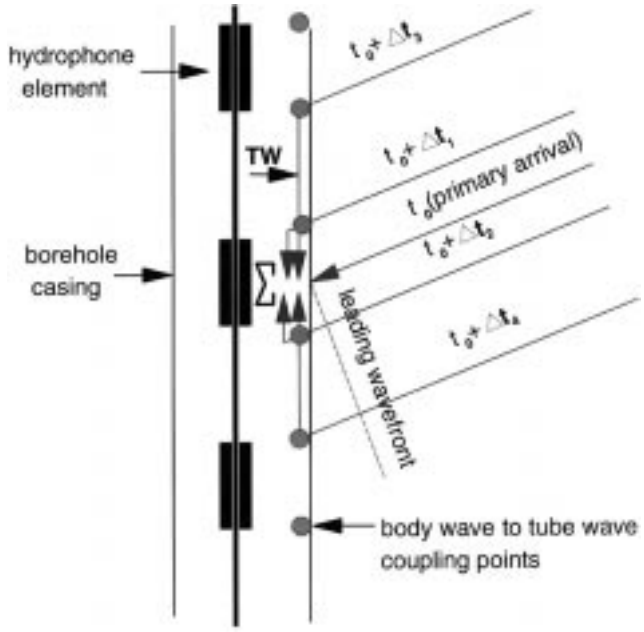

FIG. 7. Raypath diagram illustrating the first four delayed tube-wave arrivals ($t_0 + \Delta t_i$) at a hydrophone relative to the primary arrival at t_0. This occurs when the apparent velocity of the body wave exceeds that of the tube waves generated at cross-sectional area changes in the borehole fluid column. The summation ($\sum$) of the delayed tube waves with the primary arrival low-pass filters the primary waveform.

This feature may be a sand lens. Also apparent in Figure 10 is a strong reflection horizon at about 35 m. This horizon is interpreted to be the top of the Franciscan basement.

Note that the reflection image in Figure 10 is horizontally stretched by a factor of 5 : 1, with a maximum offset of 9 m. One limitation of the VSP technique is the restricted lateral coverage obtained. To insure incidence angles of less than 45°, the maximum lateral coverage cannot be more than the reflector depth, assuming a flat reflector. The overall maximum imaging offset for deep reflectors is equal to half the shot point offset distance, again assuming a flat reflector.

CONCLUSIONS

High-frequency, high-resolution (greater than 900 Hz, better than 1-m resolution) reflections from depths between 5 and 50 m were obtained using hydrophone VSP methods with foam baffles inserted between the hydrophone levels. By comparison, surface geophone data exhibited substantially lower frequency content (less than 250 Hz). Because of the shot-generated interference, surface methods were not useful for imaging reflections above 25 m at this site. On a time-per-trace basis, VSP data was acquired in substantially less time than geophone surface data.

Tube waves were the primary source of coherent noise in this VSP data. The tube waves were generated at cross-sectional area changes in the borehole fluid column. The tube waves were attenuated and slowed by the use of interhydrophone, closed-cell-foam baffles. The baffles also reduced tube-wave

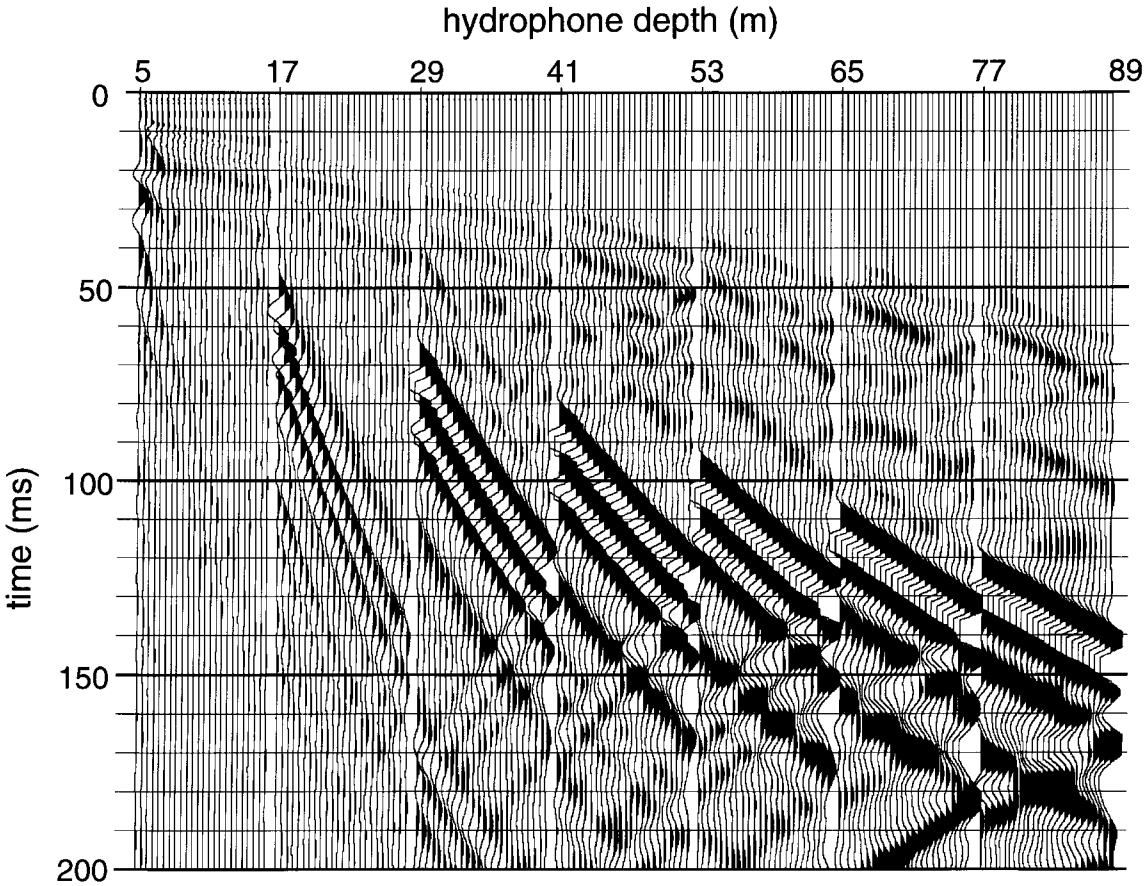

FIG. 8. VSP baffled shot records showing the effect of increasing depth on the tube-wave properties. Relative trace amplitude has been maintained. Note how tube-wave amplitude and velocity increases with depth as the closed-cell-foam baffles collapse with increasing head pressure.

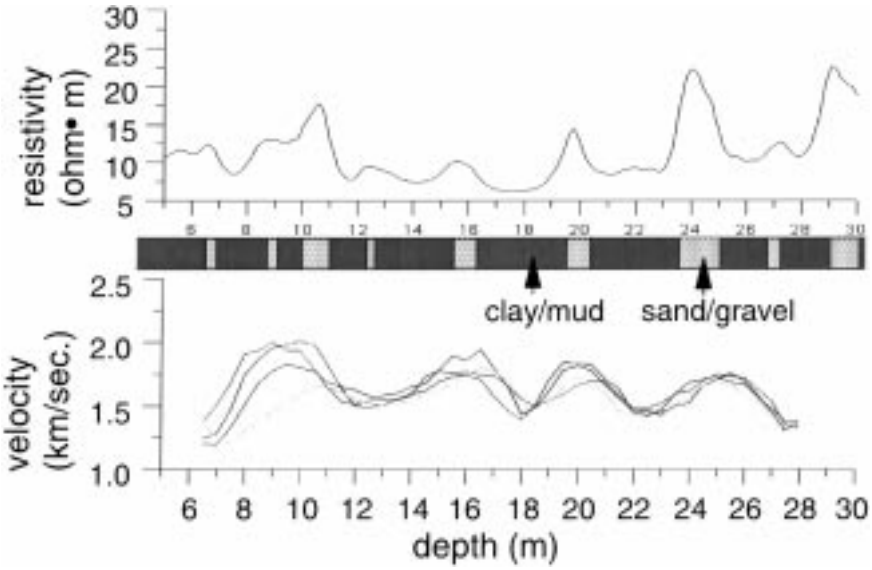

FIG. 9. *P*-wave interval velocity log obtained from VSP first-break picks, along with an induction (resistivity) log from the VSP well and a driller's lithology log from a nearby well (about 2 m away). In general, high-velocity intervals correspond with resistive (fresh water) sand and gravel units.

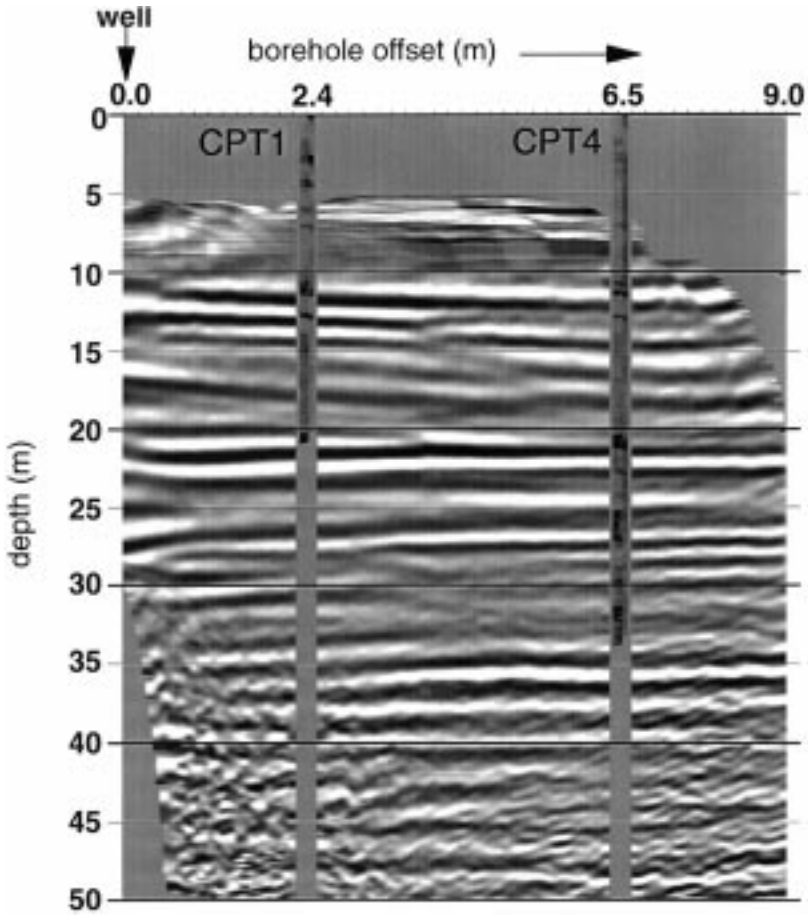

FIG. 10. Stacked reflection image after VSP-CDP mapping traces from 14 shotpoint offsets between 2.4 and 18 m. Two cone penetrometer test logs (CPT1 and CPT4), both about 1-m offline, are spliced in. Dark gray in the CPT logs indicates high-bearing load, high sleeve friction, and high resistivity, all together interpreted as fresh-water–saturated sand/gravel units.

generation and scattering from the edges of the hydrophone pods by reducing the contrast in diameter between the hydrophone pod and supporting cable. A comparison between unbaffled and baffled VSP data showed that baffling increased the usable bandwidth in the VSP data by more than 500 Hz.

Using conventional wavefield separation and VSP mapping, the multioffset VSP data was processed to produce a subsurface image. High-velocity zones (interpreted from the VSP first breaks) between 10 and 30 m were associated with gravel/sand layers in a driller's log. Several major reflection events could be correlated with thin (less than 1-m thick) gravel/sand layers, interpreted from CPT logs to be fresh water aquifers. Useful aquifer boundary information may be interpreted from the image when correlations between well log units and reflection horizons are made.

ACKNOWLEDGMENTS

This work was performed under the auspices of the U.S. Department of Energy by Lawrence Livermore National Laboratory under contract number W-7405-ENG-48.

REFERENCES

Cassell, B. R., Alam, M. A., and Millahn, K. O., 1984, Interactive VSP-CDP mapping in complex media: 54th Ann. Internat. Mtg., Soc. Expl. Geophys., Expanded Abstracts, 842–845.

Doll, W. E., Miller, R. D., and Xia, J., 1994, Non invasive shallow seismic source comparison for hazardous waste site investigations: 64th Ann. Internat. Mtg., Soc. Expl. Geophys., Expanded Abstracts, 591–594.

Glangeaud, F., and Mari, J. L., 1994, Wave separation: Éditions Technip.

Hardage, B. A., 1981, An examination of tube waves noise in vertical seismic profiling data: Geophysics, **46**, 892–903.

——— 1983, Vertical seismic profiling, part A, principles: Geophysical Press.

Hunter, J. A., Pullan, S. E., Burns, R. A., Gagne, R., and Good, R., 1984, Shallow seismic reflection mapping of the overburden bedrock interface with the engineering seismograph—some simple techniques: Geophysics, **49**, 1381–1385.

Krohn, C. E., 1984, Geophone ground coupling: Geophysics, **49**, 722–731.

Krohn, C. E., and Chen, S. T., 1992, Comparison of downhole geophones and hydrophones: Geophysics, **57**, 841–847.

Krohn, C. E., Rice, J. A., and Houston, L. M., 1991, Shallow near-surface effects on seismic waves: 61st Ann. Internat. Mtg., Soc. Expl. Geophys., Expanded Abstracts, 747–749.

Kurkjian, A. L., 1986, Theoretical far-field radiation from low-frequency horizontal acoustic point force in a vertical borehole: Geophysics, **51**, 930–939.

Lazaratos, S. K., 1993, Crosswell reflection imaging: Ph.D. thesis, Stanford University.

Marzetta, T. L., and Schoenberg, M., 1985, Tube waves in cased boreholes: 55th Ann. Internat. Mtg., Soc. Expl. Geophys., Expanded Abstracts, session BHG 2.1.

Marzetta, T. L., Orton, M., Krampe, A., Johnston, L. K., and Wuenschel, P. C., 1988, A hydrophone vertical seismic profiling experiment: Geophysics, **53**, 1437–1444.

Matsubara, Y., Kaida, Y., Osada, M., and Takaheshi, T., 1994, High resolution shallow seismic reflection profiling using portable vibrator: 64th Ann. Internat. Mtg., Soc. Expl. Geophys., Expanded Abstract, 598–601.

Payne, M. A., Eriksen, E. A., and Rape, T. D., 1994, Considerations for high resolution VSP imaging: The Leading Edge, **13**, No. 3, 173–180.

Pham, L. D., Krohn, C. E., Murray, T. J., and Chen, S. T., 1993, A tube wave suppression device for cross-well applications: 63rd Ann. Internat. Mtg., Soc. Expl. Geophys., Expanded Abstracts, 17–20.

Pouch, G. W., 1987, Hydrologic site assessment of the engineering geoscience well field at the Richmond Field Station: Ms. thesis, University of California, Berkeley.

Robertson, P. D., and Campanella, R. G., 1983, Interpretation of cone penetrometer tests—part I (sand): Can. Geotech. J., **20**, No. 4.

Steeples, D. W., Miller, R. D., and Brannan, M., 1988, Mapping bedrock as shallow as 4 m under dry alluvium with seismic reflections: 58th Ann. Internat. Mtg. Soc. Expl. Geophys., Expanded Abstracts, 88, Session ENG2.2.

Wyatt, K. D., and Wyatt, S. B., 1981, VSP-CDP mapping: Presented at the 51st Ann. Internat. Mtg. Soc. Expl. Geophys.